VirtualBrainCloud

Personalized Recommendations for Neurodegenerative Disease

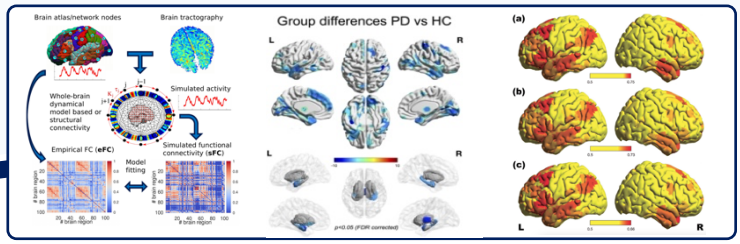

Public deliverable report

D3.10: Framework for multi-modal integrated annotations established and in use

Date	October 2021
Authors	Institute of Neuroscience and Medicine (INM-7; Brain and Behaviour) Forschungszentrum Jülich Oleksandr Popovych, Simon Eickhoff
Dissemination level:	**public**
Website	https://virtualbraincloud-2020.eu

This project has received funding from the **European Union´s Horizon 2020** research and innovation programme under **grant agreement No 826421**

Table of Contents

1. Introduction

The current deliverable is part of the VirtualBrainCloud (TVB-C/TVB-Cloud) project, which strives to leverage the potential of big data and high-performance computing (HPC) in order to develop a cloud-based brain
simulation platform for personalized prevention and treatment of neurodegenerative diseases (NDD). Very large empirical datasets, such as neuroimaging data from magnetic resonance imaging (MRI) and a variety of its modalities, collected at various sites all over the world containing data from tens of thousands of subjects, provide the basis of this huge endeavor. However, the size and complexity of such datasets come along with increased computational costs. This is aggravated by the fact that neuroimaging studies generally involve an enormous number of features. Especially in voxel-based approaches, the number of features (corresponding to the voxels of each image) vastly exceeds the number of samples (image of each subject). Therefore, the investigation of large datasets requires dimensionality reduction in many cases. This is usually done by making use of a brain atlas that provides the appropriate parcellation of the brain (Eickhoff et al., 2018; Thirion et al., 2014), in which several hundred thousand of voxels from high-resolution neuroimaging data are grouped into a few hundred brain regions. As such, they serve as biologically informed strategies of data compression, reducing the high dimensionality of neuroimaging data making them computationally better tractable and facilitating data analyses or in some cases, such as, e.g., whole-brain connectomics, even just making them possible.

Brain atlasing is central in the development of a cloud-based brain simulation platform to support personalized diagnostics and treatments in NDD, which is the ultimate goal of TVB-C/TVB-CLOUD. Advanced simulation requires an a priori parcellation of the brain into separate areas based on which individual connectomes can be established in order to simulate parcel-wise dynamics. Moreover, multi-modal atlasing functions as a scaffold that can be enriched by local annotations in form of various individual findings from brain anatomy, dynamics and pathology. As such, it serves as an integrated knowledge space, in which different kinds of information can be combined in order to obtain a more comprehensive understanding of the brain.

One approach for brain parcellation *in vivo* is resting-state functional connectivity (RSFC), which measures the synchronization of RS-fMRI signals between brain regions while the subject is resting in the scanner without performing a task (Biswal et al., 1995). This approach was applied in the Schaefer atlas (Schaefer et al., 2018), in which, at different granularity, the patterns of the RSFC were used to group the voxels (or vertices) with similar connectivity into the same parcel but at the same time assigned spatially adjacent vertices with different RSFC profiles to different parcels. Consequently, in contrast to previous publications which relied either on global similarity (clustering brain regions based on similarity in RS-fMRI time courses) or on local gradient methods (detecting abrupt transitions in functional connectivity patterns, potentially reflecting cortical areal boundaries), Schaefer combined both approaches. From a great variety of existing anatomical and functional approaches to brain parcellation (Eickhoff et al., 2018; Thirion et al., 2014), one may suppose that conceptually the Schaefer atlas might be most appropriate for investigation of the resting-state brain activity and connectivity, as tying together voxels with similar time courses optimizes the functional homogeneity of RS signals in the nodes.

In this deliverable, we demonstrate modeling of RS data by means of the Schaefer atlas, which acts as a scaffold that can be enriched by local annotations. In order to provide region-level annotations of the nodes for The Virtual Brain (TVB), we extensively developed, tested and optimized the structural and functional profiling of the regions, with a special focus on NDDs and common confounds.

2. Partners involved

This deliverable was prepared by the Institute of Neuroscience and Medicine (Brain and Behaviour, INM-7) from the Forschungszentrum Jülich (FZJ). The computational resources were provided by the JURECA computational cluster at the FZJ (Jülich Supercomputing Centre).

3. Description of work performed

3.1 Application of the Schaefer atlas in whole-brain dynamical modeling

As already stated above, brain parcellations in form of atlases are a beneficial tool for different purposes in the context of improved understanding of brain organization, predicting individual phenotypes, or precision medicine. One example is whole-brain dynamical modeling. This is necessary to develop a cloud-based brain simulation platform for personalized prevention and treatment of neurodegenerative diseases (NDD), which is the aim of TVB-C/TVB-CLOUD. Dynamical models of brain activity can be used in an attempt to explain the relationship between neuronal dynamics and neuronal structures, instead of just describing it. The procedure of the model derivation and validation involves its fitting to empirical data, where the model parameters are adapted in such a way that the model output (i.e., simulated RSFC) approximates the empirical data as much as possible. A detailed investigation of the validated models, in particular, the impact of one or another model parameter on the simulated data and its correspondence to the empirical one can contribute to the understanding of the underlying mechanisms of the observed neuronal activities. In contrast, such a freedom of the parameter variation is absent for empirical data, which makes it difficult to reveal a mechanistic origin of the relationship between brain structure and function using only the measured data (Popovych et al., 2019). Moreover, models can serve as a testbed for testing new treatments for certain neurobiological diseases to simulate their effects first before actually applying them in practice, which can contribute to a model-based optimization of therapeutic interventions.

Utilizing brain parcellation is essential for dynamical modeling of brain activity, in order to define the nodes of a network model based on the brain regions proposed by a certain atlas (Honey et al., 2009). The individual nodes can be coupled to a brain network, in which the inter-node connections are usually derived from the structural connectivity (SC) calculated from the empirical diffusion-weighted MRI data. SC serves as a proxy for physical connections between brain regions (Hagmann et al. 2010). Together, these inter-node connections constitute what is referred to as the brain's structural connectome, contributing a description of the underlying physical organization of the brain and defining the topological structure of the network model.

After setting up the network model based on the empirical SC, the next step is to compute the network's empirical neuronal activity. The empirical FC is usually calculated from the blood oxygen level-dependent (BOLD) signals inferred from RS-fMRI. For this purpose, a brain atlas (like the Schaefer atlas) is used to divide the brain into separate parcels based on which the mean BOLD signals (averaged over all voxels in each region separately) are calculated for each brain parcel. The extracted BOLD signal of each brain region (network node) is then correlated with those of all the other nodes across the brain, resulting in empirical FC matrices for each subject. One modeling approach is to simulate this empirical functional connectome. In order to do so, simulated BOLD time series are generated for each node of the derived dynamical model, which are then used to calculate the simulated FC (Honey et al., 2009).

Finally, the simulated FC has to be validated against the empirical data. Since the model comprises different parameters, like coupling strength, whose true values are unknown, these parameters have to be adjusted in the model validation step so that the model output approximates the empirical FC as closely as possible (Honey et al., 2009, Cabral et al., 2011). Once the optimal parameter values are obtained, they are fixed, and the model is supposed to be validated against empirical data. This whole process is schematically depicted in Figure 1. The model validation of one model against empirical data is displayed in Figure 2 (Popovych et al. 2021). Here, the fitting of the simulated FC to empirical FC (Fig. 2A-C) and the fitting of the simulated FC to empirical SC (Fig. 2D-F) based on the Schaefer atlas is demonstrated. The similarity between the empirical functional and structural connectomes and the simulated functional connectome in the model parameter space is represented in Figs. 2A and 2D respectively, where the optimal parameter points of the best fit are indicated by white circles. The corresponding simulated FC matrices of the best fit compared with empirical FC and empirical SC are shown in Figs. 2B and 2E, respectively, and the corresponding empirical FC matrix and empirical SC matrix are depicted in Figs. 2C and 2F, respectively.

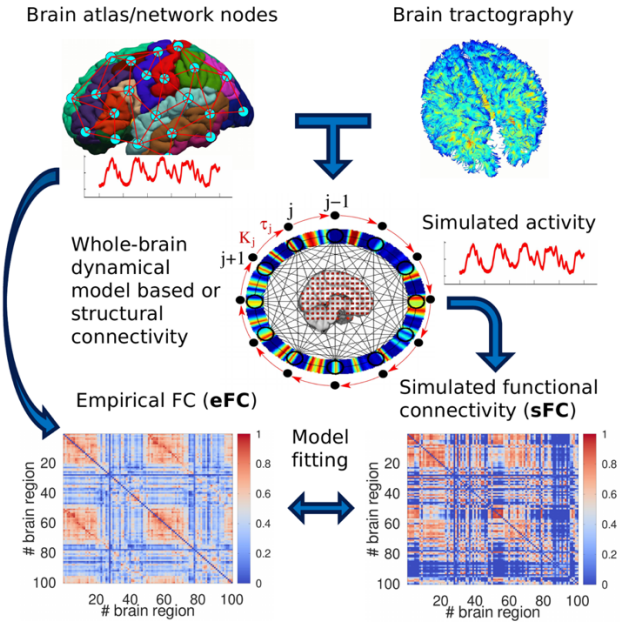

Figure 1. Derivation and validation of a whole-brain dynamical model. First, brain regions extracted from an atlas serve as nodes in the modeled network (upper left). Inter-node connections are extracted from the empirical SC calculated from dwMRI data (upper right). After that, the empirical FC (eFC) of the atlas-based network is computed via correlating each parcel's mean BOLD signal with that of the other parcels across the brain (lower left). Simulated FC (sFC) is calculated by cross-correlation of the simulated BOLD time series that are generated for each node of the derived model (lower right). Finally, the simulated model's parameters are adapted in such a way that the sFC approximates the eFC as closely as possible.

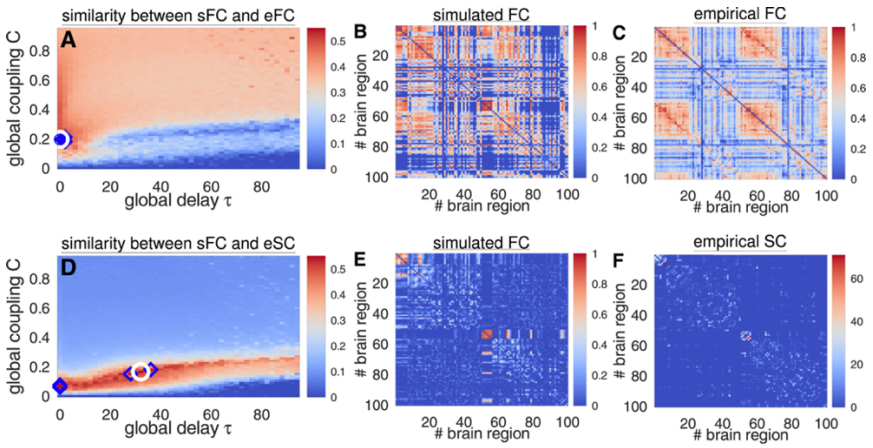

Figure 2. The model validation for one model based on Schaefer parcellation against empirical data is displayed.

3.2 Spatial annotations within the nodes of the TVB atlas scaffold

As demonstrated above, RS data can be modeled by means of the Schaefer atlas, which additionally acts as a scaffold that can be enriched by local annotations. In order to provide region-level annotations for the nodes of TVB, we extensively developed, tested and optimized the structural and functional profiling of the regions within this same scaffold. Investigating the regions defined by the Schaefer atlas more closely, we focused especially on the examination of their relation to NDDs and common confounds, which are the main focus of the research in the context of TVB-C/TVB-CLOUD.

Providing these annotations, we investigated the functional and structural properties of the brain parcels. In the first approach, RS connectomes were created based on parcellation by the Schaefer atlas. For each parcel, the subject-specific time series were extracted by averaging the BOLD signals of all voxels within each parcel, so that every parcel ends up with an individually computed signal. After that, the connectivity pattern of each parcel was computed by correlating its time series with those of all other parcels. Finally, each parcel's connectivity with the other parcels across the whole brain for each subject was used as a feature in the subsequent prediction analysis for this specific parcel.

One exemplary application of individual FC is the investigation by Weis et al. (2020) in which a machine learning approach was employed in order to evaluate how accurately a subject's sex can be classified based on his/her individual RSFC. In contrast to previous studies which assessed sex prediction accuracy based on whole-brain connectivity patterns, using parcel-wise FC based on the Schaefer atlas had two big advantages. It allowed us to circumvent the curse of dimensionality and to investigate which brain areas' connectivity patterns can classify sex most accurately, further improving the interpretation of the results and localization of the predictive brain regions. For each parcel separately, classifiers were trained to learn the relationship between each individual parcel's FC pattern and the participants' sex. After that, these classifiers were used to predict the sex of previously unseen subjects given corresponding connectivity patterns.
Although the whole-brain FC achieved a high sex prediction accuracy, accuracies weren't similarly high for all individual brain regions. Exhibiting considerable differences in sex prediction accuracies, certain brain regions' FC was most characteristically different between males and females. Figure 3 depicts the classification accuracies for the validation of the classifier within the training sample (Fig. 3a) as well as across two unrelated test samples (Figs. 3b, 3c). The most predictive parcels were located along the cingulate cortex, in the right anterior midcingulate cortex as well as the left posterior cingulate cortex. Other highly predictive parcels were located in the bilateral medial frontal cortex, in the bilateral precuneus as well as the left lateral frontal cortex, the left temporo-parietal regions, and the insula. These results demonstrate that certain parcels exhibit significantly different FC patterns between men and women. Since sex is a common confounding variable, it is highly relevant for further analyses in the framework of TVB-C/TVB-CLOUD to know which brain regions' FC differ most between the two sexes.

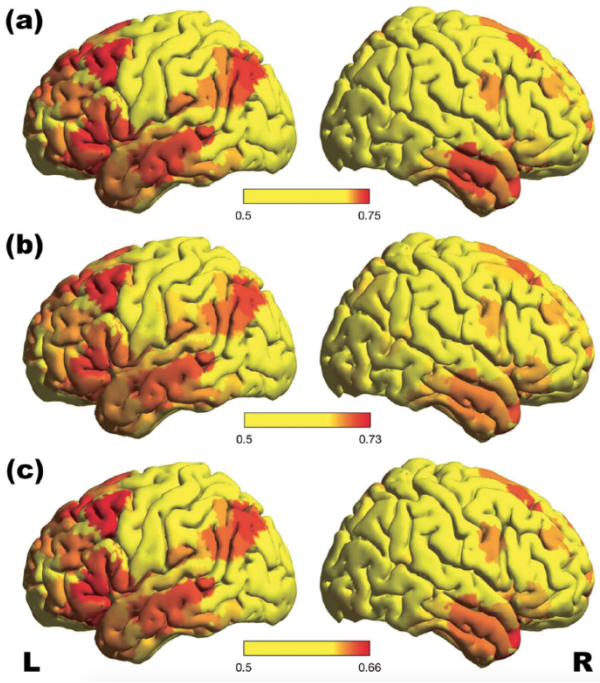

Figure 3. Classification accuracies for the validation of the classifier within the training sample (3a) as well as across two previously unknown samples (3b, 3c).

In another application, we aimed to investigate the relationship between interindividual variability in brain regions' connectivity and behavioral phenotypes (Wu et al., 2021). Therefore, we developed a connectivity-based psychometric prediction framework based on individual regions' connectivity profiles. One of the applications was to display the prediction accuracy scores distributed across all parcels, which have been defined based on the Schaefer atlas, for single psychometric variables. This means that maps were created separately for each investigated psychometric variable, depicting how accurately this variable could be predicted based on the FC of each individual brain parcel, again defined by the Schaefer atlas.

The examination of the psychometric prediction accuracy spatial distribution maps appeared to converge well with the brain mapping literature. In Figure 4 the prediction accuracy distribution maps are displayed for four psychometric variables: (Fig. 4A) motor strength; (Fig. 4B) crystallized cognition composite score; (Fig. 4C) working memory task overall accuracy; and (Fig. 4D) working memory task face condition accuracy. For example, it can be seen that the prediction accuracies for "strength" were generally low, whereas those for "working memory task overall accuracy" were quite high across the brain. Additionally, the distributions for "working memory task overall accuracy" and "working memory task face condition accuracy" were quite similar, with additional better prediction power in the right hemisphere's ventral temporal regions for the latter one, which agrees with the literature on faces processing in the brain (Sams et al. 1997; Nakamura et al. 2000; Nelson 2001). All in all, this study demonstrates that the Schaefer atlas can also be utilized to investigate how accurately different psychometric variables can be predicted based on the FC of individual pre-defined regions across the whole brain. Moreover, the results provide more insight into the task-related functions of individual brain regions whose dynamics are simulated within the scope of the TVB.

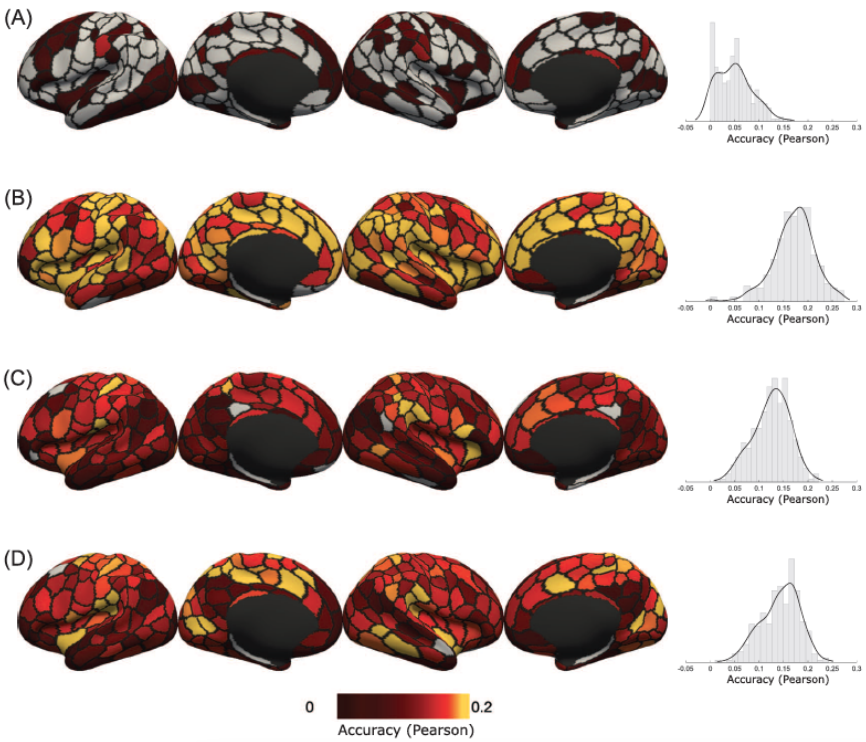

Figure 4. The prediction accuracy distribution maps of four selected psychometric variables ((A) strength; (B) crystallized cognition composite score; (C) working memory task overall accuracy; and (D) working memory task face condition accuracy) across the whole brain.

Parcellation based on the Schaefer atlas was also applied in the framework of investigating the neurobiological correlates of subtypes of neurobiological diseases. For example, Chen et al. (2020) aimed to disentangle the psychopathological heterogeneity of Schizophrenia to identify psychopathological subtypes and their neuronal representations. Therefore, we first applied machine-learning approaches to patients' scores on the Positive and Negative Syndrome Scale (PANSS; an assessment which aims to cluster schizophrenic patients into psychopathological subtypes) in order to identify its underlying generalizable factorization.

A four-factor structure was observed comprising negative, positive, affective and cognitive dimensions. Based on this four-factor structure, two core psychopathological subtypes were obtained representing the positive-negative dichotomy of this disease. Additionally, the researchers investigated how accurately patients' disease subtype membership can be predicted based on FC patterns of separate brain regions, defined by the Schaefer atlas. Therefore, we examined in how far each individual parcel's FC pattern is able to correctly assign previously unseen patients into either of the two identified disease subtypes. It was found that the individual subtype could indeed be predicted with high accuracy based on the FC patterns of the right ventromedial prefrontal cortex (vmPFC), the right temporoparietal junction (TPJ), the bilateral precuneus, and the left posterior cingulate cortex (PCC) (Figure 5), demonstrating a neurobiological divergence between the two identified psychopathological subtypes of schizophrenia. Note that this task of classifying schizophrenia subtypes is more challenging than the canonical task of classifying patients and healthy controls.

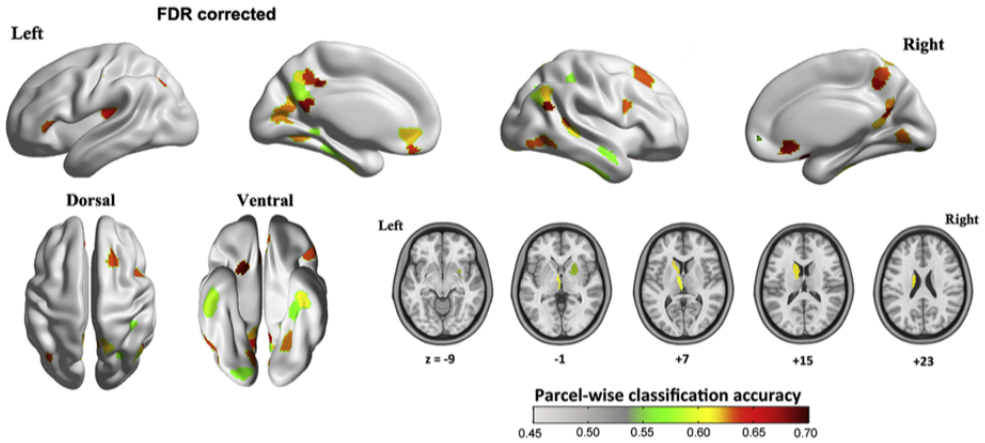

Figure 5. Classification accuracies of subtype membership based on parcel-wise FC patterns, demonstrating a neurobiological divergence between the two identified psychopathological subtypes of schizophrenia.

As already stated above, the Schaefer atlas was not only used for functional but also for structural profiling of brain regions within this same scaffold. In terms of brain anatomy, normal aging is associated with structural changes attributable to extensive gray matter (GM) atrophy (Raz et al., 2005). This is particularly true for NDDs such as Alzheimer's disease (AD), which show regional gray matter volume decline compared with age-matched healthy subjects (Ribeiro & Busatto, 2016). Moreover, previous studies found that increased atrophy rates in cognitively normal subjects are a strong indicator for the development of AD (Eskildsen et al., 2015) which indicates that structural images could be a potential biomarker for early prediction of AD onset. A widely used and valid tool to evaluate structural cerebral changes associated with normal aging or NDDs is voxel-based morphometry (VBM) which provides an automated, quantitative, and objective assessment of gray matter volume across the brain (Kurth et al., 2015). In order to investigate in which brain regions, patterns of atrophy can predict the diagnosis of NDDs, which is the ultimate goal of TVB-C/TVB-CLOUD, we first employed VBM to estimate local gray matter volume. After that, we applied brain parcellation based on the Schaefer atlas in order to calculate average gray matter volume in each individual parcel per subject to assess differences in parcel-wise atrophy patterns in healthy controls versus NDDs.

For example, Kröll et al. (2020) trained an algorithm on learning the relationship between gray matter volumes of each parcel defined by the Schaefer atlas and the presence or absence of an AD diagnosis. After that, this algorithm was used to classify previously unseen subjects as AD patients or healthy controls, given corresponding parcel-wise gray matter volumes. It was found that diagnosis could be predicted with high accuracy (91%) in previously unseen subjects. For example, the combination of patterns from the left temporal pole, the ventromedial putamen, and the right lateral prefrontal thalamus exhibited high prediction accuracy (Figure 6). Additionally, we applied the same algorithm to a new dataset to probe its prognostic capacity, which means that we evaluated whether this algorithm can predict whether a person with mild cognitive impairment (MCI) will develop AD or not. Conversion to AD was predicted with a moderate accuracy of 74%. These results serve as highly relevant local annotations within the nodes of the TVB atlas scaffold, providing information about which parcels' atrophy patterns are most predictive of a future AD diagnosis. Moreover, these atrophy patterns can be used as biomarkers to predict disease progression, which is the ultimate goal of WP 4 in TVB-C/TVB-CLOUD.

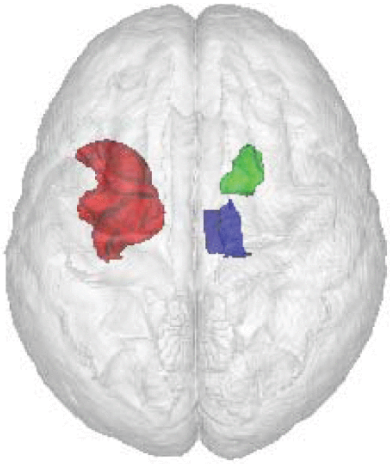

Figure 6. The combination of patterns from the left temporal pole, the ventromedial putamen, and the right lateral prefrontal thalamus exhibited high AD classification accuracy.

Another NDD investigated in TVB-C/TVB-CLOUD is Parkinson's disease (PD). In order to provide region-level annotations for this disease, Eickhoff et al. (2021) investigated atypical brain aging in PD patients as a marker of brain health. Here, machine learning models were trained to predict PD patients' chronological age using their parcel-wise patterns of regional gray matter volumes. It was found that the estimated age of PD patients based on their gray matter volume was three years higher than their true (chronological) age compared to that of healthy controls. This means that the brains of PD patients appear to be three years older compared to a healthy person of the same (chronological) age. These patients exhibited higher cortical atrophy in the right central region, medial frontal, visual and temporal cortices, the thalamus and the basal ganglia in comparison to healthy controls (Figure 7). Additionally, we correlated the accelerated aging index, i.e. the individual difference between estimated and true age, with the parcel-wise gray matter volumes of PD patients to examine which brain regions' atrophy was most strongly associated with increased brain age. The relation between increased brain age and more pronounced atrophy was strongest in the Rolandic Operculum, the cingulate cortex and visual areas (Figure 8), which deviates from the observed gray matter volume differences between PD patients and healthy controls. This indicates that the observed atrophy patterns in PD patients are only to some extend related to increased brain age. These results demonstrate which brain regions' atrophy patterns are most characteristic of increased brain age and as such serve as important regional annotations that enrich the nodes within the TVB model scaffold.

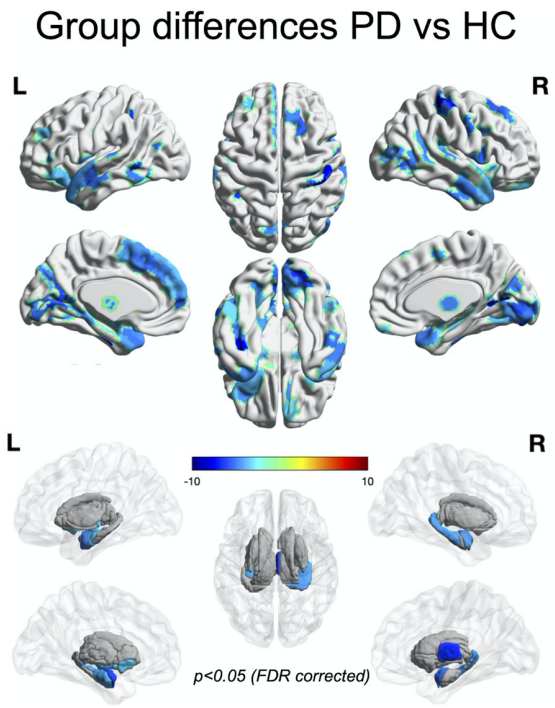

Figure 7. Differences in gray matter volume between PD patients and healthy controls. The values show the percent atrophy in patients compared to controls.

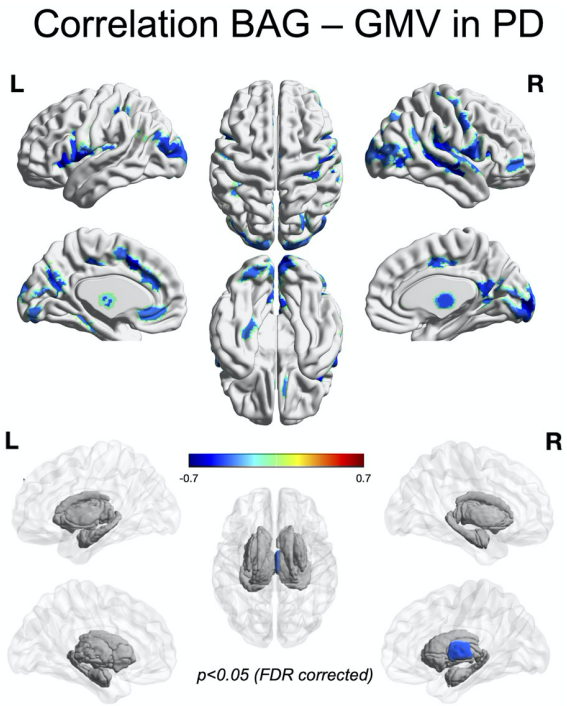

Figure 8. Correlation of the individual difference of estimated and true age with the parcel-wise gray matter volumes of PD patients.

Moreover, in the context of TVB-C/TVB-CLOUD, we aimed to investigate the predisposing risk factors of AD, indicating which people might be at greater risk of developing an NDD. Especially identifying modifiable risk factors is critical in order to postpone disease onset or slow down disease progression. One of these factors might be sleep-disordered breathing (SDB), as previous findings suggested that

patients with a certain type of SDB are more likely to develop mild cognitive impairment or dementia (Osorio et al., 2015; Yaffe et al., 2011).
Aiming to study the influence of SDB, we investigated the association between parcel-wise gray matter volumes using the Schaefer atlas and cognitive status (mild cognitive impairment versus AD versus healthy control) as well as sleep-disordered breathing (Mohajer et al.,2020). It was shown corresponding to previous findings, that the cognitive status was significantly associated with decreased gray matter volume, with patients with mild cognitive impairment and AD exhibiting lower volume in bilateral temporal lobes including fusiform gyri, medial temporal lobes, and hippocampal formations, and inferior and middle temporal lobes, as well as bilateral insula, middle frontal, and cingulate cortices, as well as left superior frontal cortex, compared to healthy controls (Figure 9). However, sleep-disordered breathing, as well as sleep-disordered breathing-by-cognitive status interaction, wasn't related to atrophy in any of the 673 parcels. This means that whereas mild cognitive impairment and Alzheimer's disease are related to increased gray matter atrophy, we observed neither a general nor a diagnostic-dependent association of sleep-disordered breathing and gray matter atrophy. These results further enrich the region-level annotations of nodes within the TVB scaffold with information about which brain regions' atrophy patterns are most related to mild cognitive impairment and AD, which is a key aspect of the research in TVB-C/TVB-CLOUD.

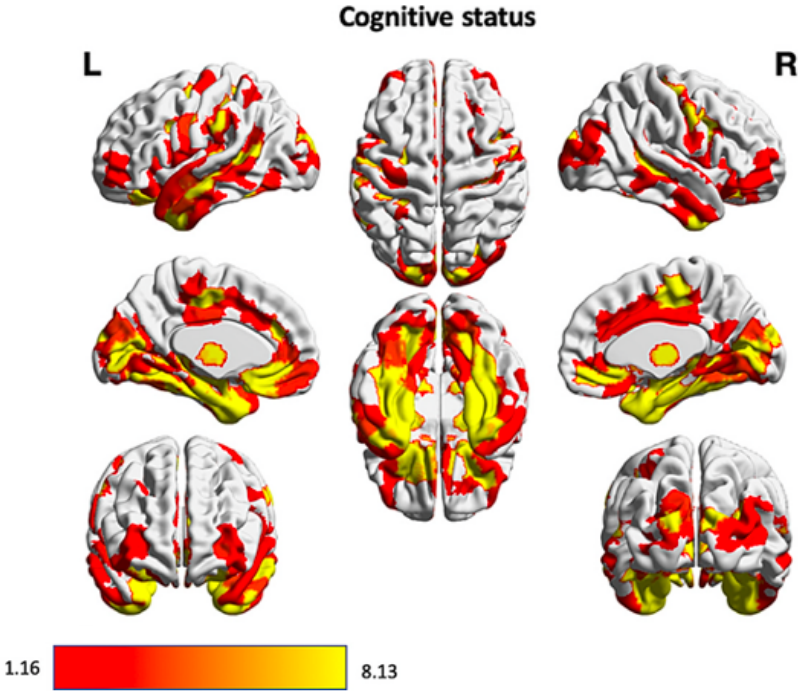

Figure 9. Association between parcel-wise gray matter volume and cognitive status of subjects.

4. Conclusion, next steps

Brain atlasing is central in the development of a cloud-based brain simulation platform to support personalized diagnostics and treatments in NDD, which is the ultimate goal of TVB-C/TVB-CLOUD. This enables the a priori parcellation of the brain into distinct, biologically meaningful regions, the dynamics of which are then simulated based on the individual connectome. Moreover, it reduces the high dimensionality of neuroimaging data features that are both more computationally manageable and yield a better ratio between the number of samples and the number of features. Additionally, it provides

a common reference system that serves as a scaffold on which local annotations based on individual findings from brain anatomy, dynamics, and pathology can be anchored.

In the past, different approaches have been evaluated in order to parcellate the brain, both structurally and functionally (Eickhoff et al., 2018; Thirion et al., 2014). From these studies, it was concluded, that the Schaefer atlas could be most appropriate for investigating the resting-state brain activity and connectivity, as it optimizes the homogeneity of the RS signals within the parcels. Based on the parcellation scheme provided by the Schaefer atlas, nodes have been extracted for whole-brain dynamic simulations within the framework of TVB-C/TVB-CLOUD. Such validated dynamical models can contribute to the understanding of the underlying mechanisms of the observed neuronal activities or they can serve as a testbed for testing new treatments for certain neurobiological diseases to simulate their effects first before actually applying them in practice, which can contribute to a model-based optimization of therapeutic interventions.

In this deliverable, we demonstrated that the Schaefer atlas serves as a scaffold to which various local annotations by means of individual findings from different studies can be added in order to gain more information about the individual regions whose dynamics are simulated within TVB-C/TVB-CLOUD. Based on this parcellation scheme, the FCs of individual parcels with all the other parcels across the brain serve as features within a prediction analysis to train an algorithm to learn the relationship between parcels' FC and for example sex classification, disease subtype prediction, or phenotype prediction. Specifically, the finding that certain parcels' FC differs between males and females is important for further analyses within the framework of TVB-C/TVB-CLOUD as sex is a common confounding variable in neuropsychological investigations. Similarly, parcel-wise gray matter volumes were used as features to train an algorithm in order to predict the age of a previously unseen participant and the presence or absence of diagnosis of an NDD like AD or PD. It was found that certain parcels' atrophy patterns can not only be used to correctly classify AD or PD patients versus healthy controls, but that they also serve as a biomarker, since they are indicative of disease progression, which is the main focus of the TVB-C/TVB-CLOUD. Moreover, evaluation of atypical brain aging in NDD patients as a marker of brain health revealed which brain regions are especially involved in increased aging.

All in all, our findings demonstrate that the Schaefer atlas is a relevant tool to parcellate RS data. Based on this parcellation, nodes were extracted to perform whole-brain dynamical simulation, which is the central approach in TVB-C/TVB-CLOUD, aiming to develop a cloud-based brain simulation platform to support personalized diagnostics and treatments in NDD. Moreover, the Schaefer atlas serves as a scaffold to which local annotations, containing information about the individual brain parcels, whose dynamics are modeled, can be added. In order to provide such regional annotations, we extensively developed, tested and optimized the structural and functional profiling of individual brain regions within this same scaffold. Here, we focused specifically on the regions' structural and functional properties in relation to diagnoses of NDD as well as common confounding variables. Doing so, we were able to provide crucial information that is linked to other work packages of the TVB-C/TVB-CLOUD, like WP4, aiming at improved diagnosis and prediction of disease progression.

5. References

Biswal, B., Zerrin Yetkin, F., Haughton, V. M., & Hyde, J. S. (1995). Functional connectivity in the motor cortex of resting human brain using echo-planar MRI. *Magnetic resonance in medicine*, *34*(4), 537-541.

Buckner, R. L., Krienen, F. M., Castellanos, A., Diaz, J. C., & Yeo, B. T. (2011). The organization of the human cerebellum estimated by intrinsic functional connectivity. *Journal of neurophysiology*, *106*(5), 2322-2345.

Cabral, J., Hugues, E., Sporns, O., & Deco, G. (2011). Role of local network oscillations in resting-state functional connectivity. *Neuroimage*, *57*(1), 130-139.

Chen, J., Patil, K. R., Weis, S., Sim, K., Nickl-Jockschat, T., Zhou, J., ... & Visser, E. (2020). Neurobiological divergence of the positive and negative schizophrenia subtypes identified on a new factor structure of psychopathology using non-negative factorization: an international machine learning study. *Biological psychiatry*, *87*(3), 282-293.

Eickhoff, C. R., Hoffstaedter, F., Caspers, J., Reetz, K., Mathys, C., Dogan, I., ... & Eickhoff, S. B. (2021). Advanced brain ageing in Parkinson's disease is related to disease duration and individual impairment. *Brain communications*, *3*(3), fcab191.

Eickhoff, S. B., Yeo, B. T., & Genon, S. (2018). Imaging-based parcellations of the human brain. *Nature Reviews Neuroscience*, *19*(11), 672-686.

Eskildsen, S. F., Coupé, P., Fonov, V. S., Pruessner, J. C., Collins, D. L., & Alzheimer's Disease Neuroimaging Initiative. (2015). Structural imaging biomarkers of Alzheimer's disease: predicting disease progression. *Neurobiology of aging*, *36*, 23-31.

Fan, L., Li, H., Zhuo, J., Zhang, Y., Wang, J., Chen, L., ... & Jiang, T. (2016). The human brainnetome atlas: a new brain atlas based on connectional architecture. *Cerebral cortex*, *26*(8), 3508-3526.

Fjell, A. M., McEvoy, L., Holland, D., Dale, A. M., Walhovd, K. B., & Alzheimer's Disease Neuroimaging Initiative. (2014). What is normal in normal aging? Effects of aging, amyloid and Alzheimer's disease on the cerebral cortex and the hippocampus. Progress in neurobiology, 117, 20-40.

Hagmann, P., Cammoun, L., Gigandet, X., Gerhard, S., Grant, P. E., Wedeen, V., ... & Sporns, O. (2010). MR connectomics: principles and challenges. *Journal of neuroscience methods*, *194*(1), 34-45.

Honey, C. J., Sporns, O., Cammoun, L., Gigandet, X., Thiran, J. P., Meuli, R., & Hagmann, P. (2009). Predicting human resting-state functional connectivity from structural connectivity. *Proceedings of the National Academy of Sciences*, *106*(6), 2035-2040.

Kröll, J. P., Eickhoff, S. B., Hoffstaedter, F., & Patil, K. R. (2020, July). Evolving complex yet interpretable representations: application to Alzheimer's diagnosis and prognosis. In *2020 IEEE Congress on Evolutionary Computation (CEC)* (pp. 1-8). IEEE.

Kurth, F., Luders, E., & Gaser, C. (2015). Voxel-based morphometry. *Brain Mapping*, ed. W. Toga (Waltham, MA: Academic Press), 345–349.

Mohajer, B., Abbasi, N., Mohammadi, E., Khazaie, H., Osorio, R. S., Rosenzweig, I., ... & Alzheimer's

Disease Neuroimaging Initiative. (2020). Gray matter volume and estimated brain age gap are not linked with sleep-disordered breathing. *Human brain mapping*, *41*(11), 3034-3044.

Nakamura, K., Kawashima, R., Sato, N., Nakamura, A., Sugiura, M., Kato, T., ... & Zilles, K. (2000). Functional delineation of the human occipito-temporal areas related to face and scene processing: a PET study. *Brain*, *123*(9), 1903-1912.

Nelson, C. A. (2001). The development and neural bases of face recognition. *Infant and Child Development: An International Journal of Research and Practice*, *10*(1-2), 3-18.

Osorio, R. S., Gumb, T., Pirraglia, E., Varga, A. W., Lu, S. E., Lim, J., ... & Alzheimer's Disease Neuroimaging Initiative. (2015). Sleep-disordered breathing advances cognitive decline in the elderly. Neurology, 84(19), 1964-1971.

Popovych, O. V., Jung, K., Manos, T., Diaz-Pier, S., Hoffstaedter, F., Schreiber, J., ... & Eickhoff, S. B. (2021). Inter-subject and inter-parcellation variability of resting-state whole-brain dynamical modeling. *NeuroImage*, 118201.

Popovych, O. V., Manos, T., Hoffstaedter, F., & Eickhoff, S. B. (2019). What can computational models contribute to neuroimaging data analytics?. *Frontiers in systems neuroscience*, *12*, 68.

Raz, N., Lindenberger, U., Rodrigue, K. M., Kennedy, K. M., Head, D., Williamson, A., ... & Acker, J. D. (2005). Regional brain changes in aging healthy adults: general trends, individual differences and modifiers. Cerebral cortex, 15(11), 1676-1689.

Ribeiro, L. G., & Busatto, G. (2016). Voxel-based morphometry in Alzheimers disease and mild cognitive impairment: Systematic review of studies addressing the frontal lobe. Dementia & neuropsychologia, 10, 104-112.

Sams, M., Hietanen, J. K., Hari, R., Ilmoniemi, R. J., & Lounasmaa, O. V. (1997). Face-specific responses from the human inferior occipito-temporal cortex. *Neuroscience*, *77*(1), 49-55.

Schaefer, A., Kong, R., Gordon, E. M., Laumann, T. O., Zuo, X. N., Holmes, A. J., ... & Yeo, B. T. (2018). Local-global parcellation of the human cerebral cortex from intrinsic functional connectivity MRI. *Cerebral cortex*, *28*(9), 3095-3114.

Thirion, B., Varoquaux, G., Dohmatob, E., & Poline, J. B. (2014). Which fMRI clustering gives good brain parcellations?. *Frontiers in neuroscience*, *8*, 167.

Weis, S., Patil, K. R., Hoffstaedter, F., Nostro, A., Yeo, B. T., & Eickhoff, S. B. (2020). Sex classification by resting state brain connectivity. *Cerebral cortex*, *30*(2), 824-835.

Wu, J., Eickhoff, S. B., Hoffstaedter, F., Patil, K. R., Schwender, H., Yeo, B. T., & Genon, S. (2021). A Connectivity-based Psychometric Prediction Framework for Brain-behavior Relationship Studies. *bioRxiv*, 2020-01.

Yaffe, K., Laffan, A. M., Harrison, S. L., Redline, S., Spira, A. P., Ensrud, K. E., ... & Stone, K. L. (2011). S Sleep-disordered breathing, hypoxia, and risk of mild cognitive impairment and dementia in older women. Jama, 306(6), 613-619.